ORIGINAL RESEARCH

# A Novel *In Vitro* Human Granuloma Model of Sarcoidosis and Latent Tuberculosis Infection

Elliott D. Crouser[1]*, Peter White[2]*, Evelyn Guirado Caceres[3], Mark W. Julian[1], Audrey C. Papp[4], Landon W. Locke[3], Wolfgang Sadee[4], and Larry S. Schlesinger[3]

[1]Division of Pulmonary, Allergy, Critical Care, and Sleep Medicine, the Dorothy M. Davis Heart and Lung Research Institute, the Ohio State University Wexner Medical Center, Columbus, Ohio; [2]Center for Microbial Pathogenesis, the Research Institute at Nationwide Children's Hospital, Columbus, Ohio; and [3]Department of Microbial Infection and Immunity, Center for Microbial Interface Biology, and [4]Department of Cancer Biology and Genetics, the Ohio State University Wexner Medical Center, Columbus, Ohio

ORCID ID: 0000-0003-3197-6746 (E.D.C.).

## Abstract

Many aspects of pathogenic granuloma formation are poorly understood, requiring new relevant laboratory models that represent the complexity (genetics and diversity) of human disease. To address this need, we developed an *in vitro* model of granuloma formation using human peripheral blood mononuclear cells (PBMCs) derived from patients with active sarcoidosis, latent tuberculosis (TB) infection (LTBI), or normal healthy control subjects. PBMCs were incubated for 7 days with uncoated polystyrene beads or beads coated with purified protein derivative (PPD) or human serum albumin. In response to PPD-coated beads, PBMCs from donors with sarcoidosis and LTBI formed robust multicellular aggregates resembling granulomas, displaying a typical T-helper cell type 1 immune response, as assessed by cytokine analyses. In contrast, minimal PBMC aggregation occurred when control PBMCs were incubated with PPD-coated beads, whereas the response to uncoated beads was negligible in all groups. Sarcoidosis PBMCs responded to human serum albumin–coated beads with modest cellular aggregation and inflammatory cytokine release. Whereas the granuloma-like aggregates formed in response to PPD-coated beads were similar for sarcoidosis and LTBI, molecular profiles differed significantly. mRNA expression patterns revealed distinct pathways engaged in early granuloma formation in sarcoidosis and LTBI, and they resemble molecular patterns reported in diseased human tissues. This novel *in vitro* human granuloma model is proposed as a tool to investigate mechanisms of early granuloma formation and for preclinical drug discovery research of human granulomatous disorders.

Clinical trial registered with www.clinicaltrials.gov (NCT01857401).

**Keywords:** AmpliSeq; peripheral blood mononuclear cell; purified protein derivative; RNA-Seq; Th1

## Clinical Relevance

We have developed an "*in vitro* human model of granuloma formation," which is shown to recapitulate molecular mechanisms that have been established in corresponding diseased human tissues. The model is unique in that it allows us to explore the mechanisms of early granuloma formation, which is critical for determining disease phenotype and is not represented in human tissue samples. The *in vitro* model is readily adopted in most laboratories, requires minimal risk to the study subjects, and represents the complex genetics of each disease, features which have not been accurately modeled in animals. The model can be used for biomarker discovery, exploration of disease mechanisms, and for preclinical testing of novel therapeutics.

(Received in original form October 4, 2016; accepted in final form May 18, 2017)

*These authors contributed equally to the preparation of the manuscript.

This work was supported by the National Institutes of Health through the Ohio State University Center for Clinical and Translational Science Award (CTSA) grant UL1TR001070 (E.D.C. and L.S.S.) and grant U01GM092655 (W.S.).

Author Contributions: Conception and design—E.D.C., P.W., E.G.C., M.W.J., L.W.L., W.S., and L.S.S.; analysis and interpretation—E.D.C., P.W., E.G.C., M.W.J., A.C.P., L.W.L., W.S., and L.S.S.; drafting the manuscript for important intellectual content—E.D.C., P.W., E.G.C., M.W.J., W.S., and L.S.S.

Correspondence and requests for reprints should be addressed to Elliott D. Crouser, M.D., Division of Pulmonary, Allergy, Critical Care and Sleep Medicine, the Ohio State University Wexner Medical Center, Room 201F, the Davis Heart & Lung Research Institute, 473 West 12th Avenue, Columbus, OH 43210. E-mail: crouser.1@osu.edu

This article has an online supplement, which is accessible from this issue's table of contents at www.atsjournals.org

Am J Respir Cell Mol Biol Vol 57, Iss 4, pp 487–498, Oct 2017

Originally Published in Press as DOI: 10.1165/rcmb.2016-0321OC on June 9, 2017
Internet address: www.atsjournals.org

Progress in the field of granulomatous disease research is currently hindered by the lack of models that accurately replicate the complex genetics and multicellular immune responses characterizing the corresponding human conditions. The resultant reliance on human tissues for research relating to granulomatous infections or granulomatous disorders of noninfectious etiology (e.g., sarcoidosis) greatly increases the research cost and limits dynamic interrogation, efficiency, and reproducibility of the research. In 2004, an NHLBI working group on future directions in sarcoidosis research concluded that relevant laboratory models of sarcoidosis are needed to "…elucidate the underlying mechanisms, including predisposing factors, and defective immune responses" characteristic of the disease (1). Likewise, new laboratory models of tuberculosis (TB) are needed to expedite preclinical testing of novel therapies and better understand host–pathogen interactions (2, 3). However, no widely accepted animal or *in vitro* models have been developed to date.

Historically, rodent models were favored for studying human diseases; however, by and large, these models have not been suitable for investigating human granulomatous disorders. Rodent models, including genetically modified mice, are limited by an inability to accurately replicate polygenic immune-mediated human granulomatous diseases. Significant challenges also arise with humanized mouse models, wherein immune cell progenitors are introduced from human donors to replicate the complex genetic traits of diseased humans, because the engraftment of the human immune system is often incomplete or is associated with abnormal inflammatory cell activation (4). As a result of these and other practical limitations, prior attempts to model human granulomatous disorders, such as sarcoidosis or latent TB infection (LTBI), in rodents have not gained wide acceptance (5, 6). For example, attempts to sensitize mice to immunogenic TB antigens lead to self-limited granuloma formation, which equates to a normal Th1 immune response (5). By contrast, patients with sarcoidosis develop sustained and, in some cases, progressive granulomatous inflammation in response to TB and presumably other environmental antigens (7). Moreover, granuloma formation and related disease manifestations in murine TB models differs significantly from the human condition (8), and LTBI, common in humans, is not observed in rodents (6). Thus, animal models are largely not reliable surrogates for human granulomatous diseases.

Recent studies show that peripheral blood mononuclear cells (PBMCs) derived from patients with LTBI or active TB form granulomas *in vitro* in response to TB antigen challenge (9, 10). This should come as no surprise, given the evidence that granulomas are assembled and maintained through the recruitment of circulating immune cells (11, 12). These results indicate that PBMCs derived from patients with sarcoidosis, LTBI, and other granulomatous disorders manifest the complex and, as yet, undefined genetic features that predispose to these disorders, and could serve as a tractable *in vitro* model of granulomatous diseases.

Sarcoidosis and LTBI are examples of human disorders representing the opposite ends of a spectrum of granulomatous responses to common antigens. Specifically, patients with sarcoidosis who are naive to TB infection often manifest with abnormally intense Th1 immune responses to TB antigens (13), whereas LTBI is characterized by an impaired Th1 immune response to TB antigens, leading to failure to fully resolve the infection (14). Thus, we sought to determine whether PBMCs from patients with sarcoidosis and LTBI form granulomas in response to tuberculin purified protein derivative (PPD), and, if so, whether the granulomas conform to established characteristics of tissue granulomas in corresponding human disease, the ultimate goal being to develop a novel *in vitro* research model for granulomatous disorders.

**Table 1.** Patient Demographics

| Groups | Age (*Yr*) | Race (*W/B/O*) | Sex (*M/F*) |
|---|---|---|---|
| Control ($n = 5$) | 28.0 ± 2.5 | 3/0/2 | 3/2 |
| LTBI ($n = 5$) | 28.6 ± 3.9 | 1/1/3 | 3/2 |
| Sarcoidosis ($n = 6$) | 49.8 ± 6.4 | 4/2/0 | 2/4 |

*Definition of abbreviations*: LTBI, latent tuberculosis infection; W/B/O, white/black/other.

## Materials and Methods

Please refer to the online supplement for additional methodological details.

### Human Blood Samples

With Institutional Review Board (The Ohio State University, Columbus, Ohio; no. 2014H0380) approval and informed, written consent, blood samples were obtained from three study groups: (*1*) six patients with active pulmonary sarcoidosis being TB skin test and/or IFN-γ release assay (IGRA) negative using the Quantiferon test; (*2*) five subjects with LTBI having a positive PPD skin and/or Quantiferon test, no clinical symptoms, and absent chest radiographic evidence of active TB infection; and (*3*) five matching disease-free, TB skin test and/or Quantiferon-negative control subjects.

**Table 2.** Disease Characteristics Patients with Sarcoidosis

| Patient* | Scadding Stages I–IV | Extrathoracic Organ Involvement | Lymphopenia <1,200/μl |
|---|---|---|---|
| SARC11 | IV | | Yes |
| SARC12 | II | | No |
| SARC13 | I | Skin | No |
| SARC14 | I | Stomach | Yes |
| SARC16 | II | | No |
| SARC17 | III | Skin | Yes |

*As identified in Figures 3 and 4. Because of a very limited obtained blood sample, SARC15 failed to yield enough peripheral blood mononuclear cells to perform the experiments and was not included.

### PPD- and Human Serum Albumin–Coated Bead Preparation

Fluoresbrite carboxylated microspheres (bright blue fluorescence, 1.0 μm) were either resuspended in PBS or covalently coupled to select proteins (i.e., PPD, human serum albumin [HSA]) via the carbodiimide method (*see* Figures E1 and E2 and further description in the online supplement). Prepared beads were diluted into RPMI media and added to isolated PBMCs at a multiplicity of infection of 50:1 relative to the number of monocytes/macrophages present.

### PBMC Isolation from Human Blood and Culture Conditions

Human PBMCs were isolated from whole-blood samples employing Ficoll-Paque PLUS (GE Healthcare Bio-Sciences, Piscataway, NJ) as previously described (10) and detailed further in the online supplement. PBMCs ($2 \times 10^6$ cells/ml) were cultured for 7 days in RPMI 1,640 medium containing 10% human AB serum and each of the following separate treatments: (*1*) volume-matched vehicle control; (*2*) uncoated (PBS-washed) beads; (*3*) HSA-coated beads; or (*4*) PPD-coated beads.

### Measuring *In Vitro* Granuloma-Like Cell Aggregates

The stage of granuloma formation (granuloma index) was determined semiquantitatively at Day 7 after treatment for each treatment in each group, as described in the online supplement and Figure E3. The scoring system is based on published literature and established models (9, 10, 15), where there is a progressive increase in the size and specific cell distribution of the granulomas.

### Cytokine Analysis

Human PBMC–cleared supernatants, collected 7 days after treatment, were analyzed for their granulocyte-macrophage colony–stimulating factor (GM-CSF), IFN-γ, IL-2, IL-10, IL-12p40/IL-23, IL-12p70, IL-13, and TNF-α concentrations by ELISA, according to the manufacturer's recommendations (IFN-γ, IL-10, IL-12p70, IL-13, TNF-α [eBioscience, Inc., San Diego, CA], GM-CSF, IL-2, and IL-12p40/IL-23 [BioLegend, San Diego, CA]).

### Granuloma Gene Expression Analysis

Granuloma cells were harvested into TRIzol reagent (Ambion, Life Technologies, Carlsbad, CA). Total RNA was purified and DNase treated using the SpinSmart RNA purification kit (Denville Scientific, Inc., Holliston, MA), according to the manufacturer's protocol. Ion Torrent AmpliSeq Transcriptome Human Gene Expression kit (Thermo Fisher Scientific, Inc., Pittsburgh, PA) was used to prepare libraries from 10 ng granuloma RNA. Quantified barcoded libraries were combined in equal amounts for emulsion PCR on the Ion OneTouch2 instrument (Thermo Fisher Scientific, Inc.). Templated libraries were loaded onto Ion PI Chips and sequenced on the Ion Proton Sequencer, using the Ion PI Sequencing 200 Kit v2 reagents (Thermo Fisher Scientific, Inc.). Transcript quantification was performed with the mm Hgent Suite (Thermo Fisher Scientific, Inc.) analysis plugin, "AmpliSeqRNA".

AmpliSeq gene expression data were normalized and postalignment statistical analyses performed using *DESeq2* (16), with custom analysis scripts written in R. Comparisons of gene expression and associated statistical analyses were made between different conditions of interest, as presented subsequently here, using the normalized read counts. Transcripts

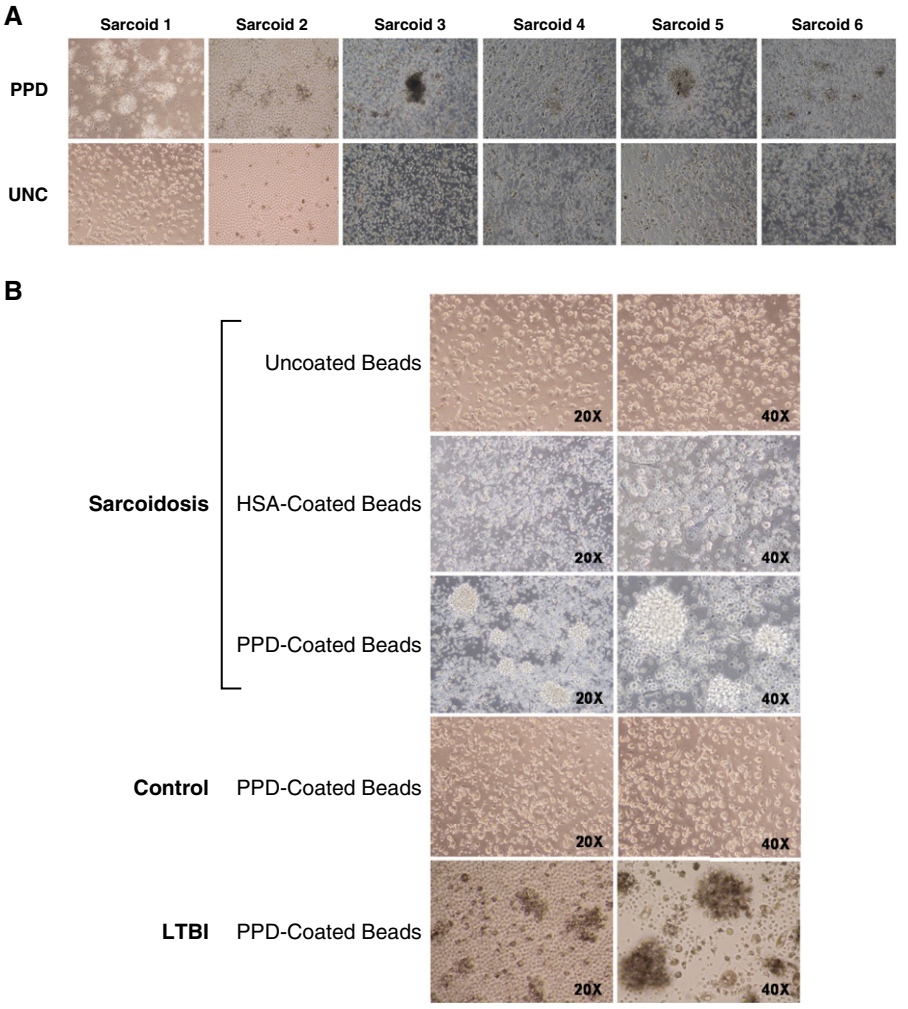


**Figure 1.** *In vitro* granuloma-like cell aggregate formation induced by purified protein derivative (PPD)–stimulated peripheral blood mononuclear cells (PBMCs) of patients with sarcoidosis and latent tuberculosis (TB) infection (LTBI). (*A*) Representative light photomicrographs (×20) obtained 7 days after sarcoidosis PBMCs were incubated with PPD-coated (PPD) or uncoated (UNC) beads. (*B*) Representative light photomicrographs (×20 and ×40, respectively) obtained 7 days after the indicated treatment of PBMCs in the sarcoidosis, LTBI, and control groups. Uncoated beads elicited no significant cellular aggregation in any of the study groups, and human serum albumin (HSA)–coated beads caused no perceptible aggregation in any group, with the exception of the sarcoidosis group, in which an intermediate response was observed. PPD-coated beads induced prominent cellular aggregation in the sarcoidosis and LTBI groups but not in the control subjects.

were considered to be significantly differentially expressed using a 10% false discovery rate (DESeq2-adjusted $P \leq 0.05$) and a fold-change cut-off of 2 between the uncoated bead–treated and PPD-treated samples.

## Results

### Study Subjects

The study was approved by the local institutional review board and was listed with the National Institutes of Health (ClinicalTrials.gov identifier: NCT01857401). Inclusion criteria for subjects with sarcoidosis were based upon the accepted standards (biopsy-proven noncaseating granulomatous tissue inflammation in the absence of other likely causes) (17), and all patients had evidence of active (nonfibrotic) lung disease and negative screening for LTBI (negative PPD skin test and/or negative IGRA). LTBI was characterized by a positive PPD skin test and/or positive IGRA with no signs or symptoms of active disease (e.g., fevers, cough, night sweats). All study participants provided informed, written consent. The demographic features of the study subjects are summarized in Table 1. Of note, none of the study subjects were active smokers or were being actively treated with immune suppressants. Additional information pertaining to the disease characteristics of the patients with sarcoidosis is provided in Table 2.

### *In Vitro* Cell Aggregation Resembling Granulomas

Control subjects, subjects with sarcoidosis, and those with LTBI demonstrated minimal cellular aggregation in response to beads alone. By contrast, treatment with PPD-coated beads elicited the formation of multicellular (granuloma-like) complexes in PBMCs derived from patients with sarcoidosis and LTBI, whereas comparatively minimal cell aggregation was apparent under these conditions in normal healthy control subjects (Figures 1 and Figure E3). In response to HSA-coated beads, patients with sarcoidosis displayed an intermediate cellular aggregation response (Figure 1), with comparatively minimal responses in LTBI and control subjects (data not shown). Immunofluorescence (*see* the online supplement for methods and antibodies used) of granuloma-like structures 7 days after PPD-coated bead stimulation in both patients with LTBI and those with sarcoidosis demonstrated the predominant presence of both centrally clustered macrophages and peripherally situated lymphocytes (Figure 2; cellular components [with isotype control antibodies] and three-dimensional video views of the granuloma shown in Figures E4 and E5, respectively).

### Extracellular Cytokine and Chemokine Profiles

Release of Th1-related cytokines, chemokines, and growth factors (IFN-γ, IL-2, IL-12p40, IL-13, GM-CSF, and TNF-α) increased, as expected, in response to PPD-coated beads in all treatment groups (Figure 3 and Figure E6). However, release of IFN-γ was significantly lower in subjects with sarcoidosis compared with those with subjects with LTBI or control subjects, whereas TNF-α release was significantly

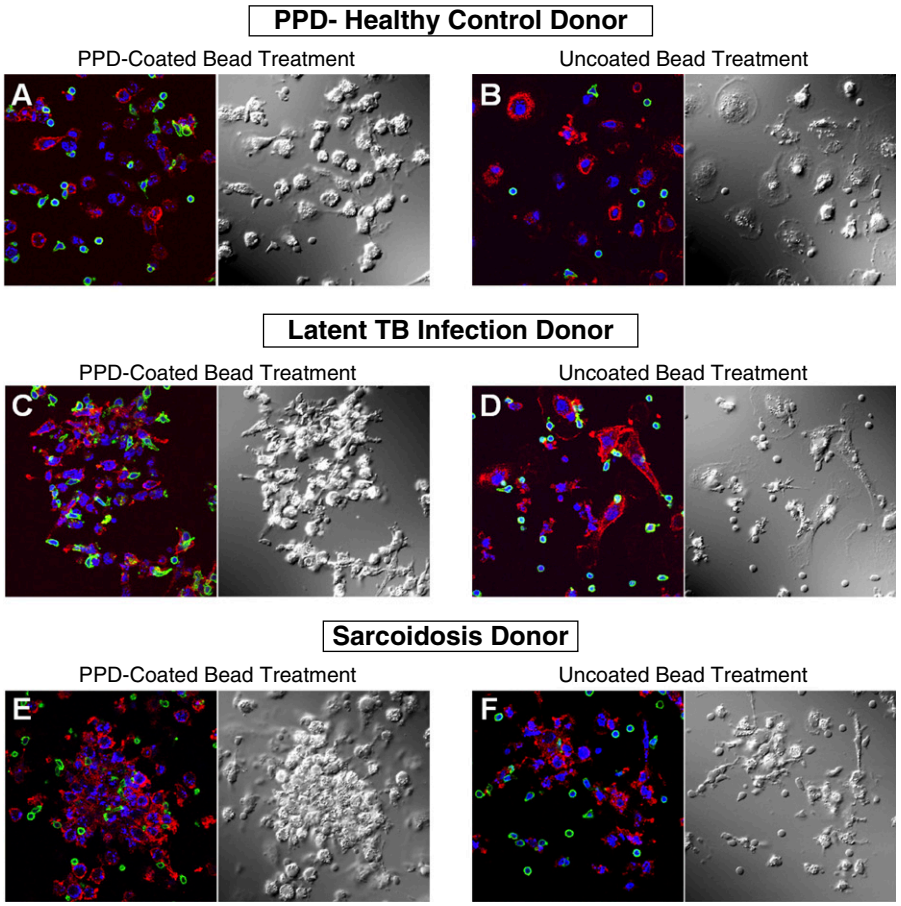


**Figure 2.** Composite immunofluorescence imaging of granuloma-like structures demonstrates the presence of both macrophages and lymphocytes. Representative photomicrographs of immunostained PBMCs in granuloma-like structures 7 days after bead treatment using confocal microscopy. Composite images of 4′,6-diamidino-2-phenylindole, CD11b, and CD3 are shown in *blue*, *red*, and *green*, respectively. (*A*) PPD-coated and (*B*) uncoated bead–stimulated PBMCs obtained from a $PPD^-$, healthy control subject showing $CD11b^+$ macrophages and $CD3^+$ lymphocytes in the absence of granuloma formation. (*C* and *D*) $CD11b^+$ macrophages and $CD3^+$ lymphocytes in a granuloma-like structure of cells obtained from a subject with LTBI after PPD-coated and uncoated bead stimulation, respectively. (*E* and *F*) $CD11b^+$ macrophages and $CD3^+$ lymphocytes in a granuloma-like structure of cells obtained from a patient with sarcoidosis after PPD-coated and uncoated bead stimulation, respectively. Uncoated beads did not induce granuloma-like structures in both the patients with LTBI and those with sarcoidosis. In each *panel*, a matching differential interference contrast image is shown next to each composite image. All images were acquired at ×60 magnification.

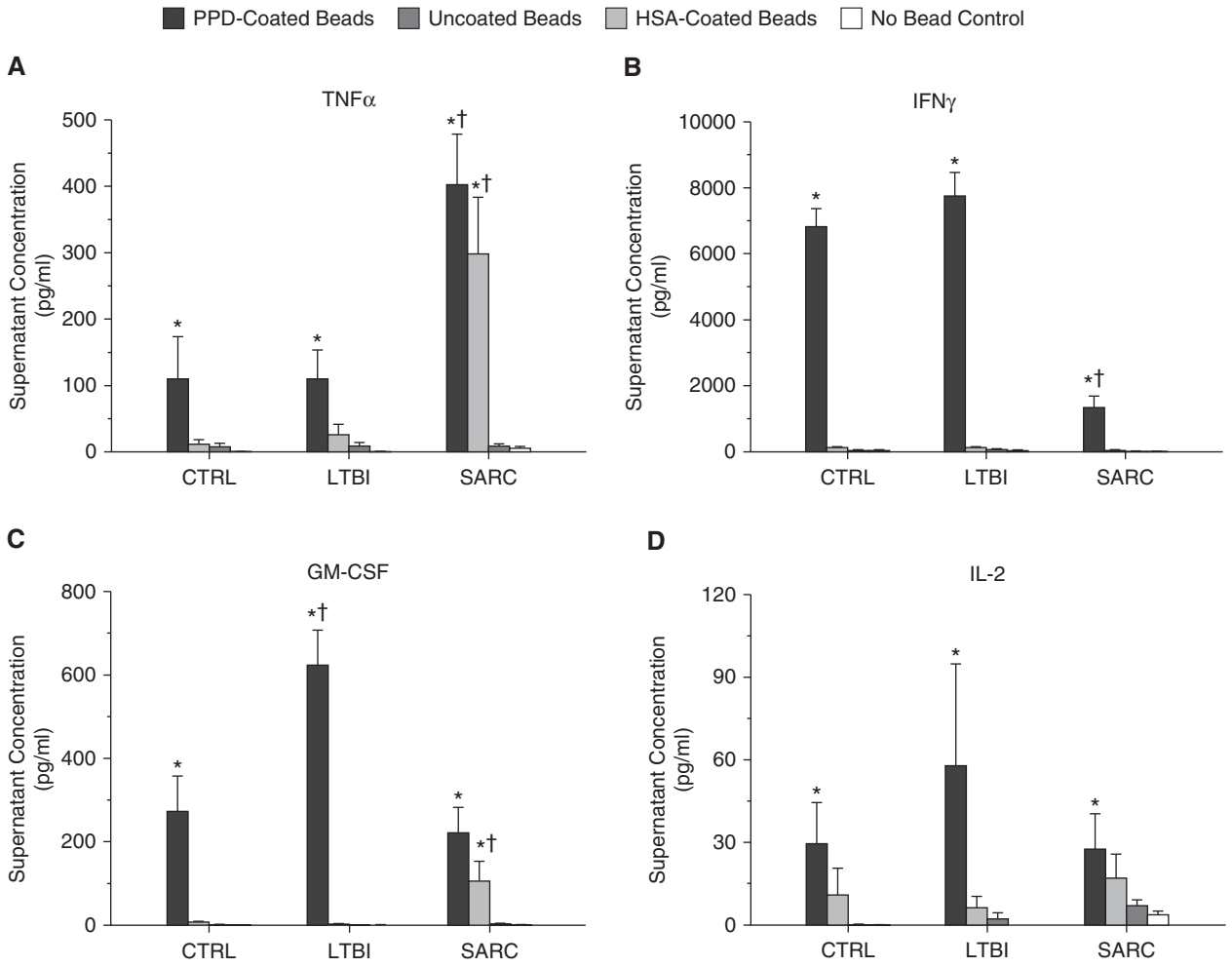


**Figure 3.** Extracellular cytokine release from PPD-stimulated PBMCs revealed distinct patterns in sarcoidosis and LTBI. Compared with treatment with uncoated or HSA-coated beads, incubation of PBMCs in the sarcoidosis (SARC), LTBI, and control (CTRL) groups with PPD-coated beads for 7 days was associated with a significant increase in the extracellular release of T helper type 1 cytokines (IFN-γ [*B*], IL-2 [*D*]) and other proinflammatory cytokines (TNF-α [*A*], granulocyte–macrophage colony-stimulating factor [GM-CSF] [C]). Treatment of sarcoidosis PBMCs with HSA-coated beads induced a significant increase in TNF-α and GM-CSF release compared with HSA-coated bead treatment of PBMCs from the LTBI or control groups (*$P < 0.05$, compared with the corresponding [within group] uncoated and no bead controls; †$P < 0.05$, relative to the matching [between groups] bead treatments).

higher in subjects with sarcoidosis compared with those with LTBI or control subjects. HSA-coated beads elicited an immune response corresponding to selective monocyte/macrophage activation (GM-CSF, TNF-α) in patients with sarcoidosis (Figure 3). This response to HSA-coated beads was not observed in either subjects with LTBI or control subjects.

### Gene Expression Analysis

One sample each from the LTBI and control groups had inadequate RNA quality and were excluded from AmpliSeq analysis (control, $n = 4$; LTBI, $n = 4$; sarcoidosis, $n = 6$). In separate quality-control assays, AmpliSeq data were highly reproducible (technical replicates with $r = \sim 0.99$ and biological replicates with $r > \sim 0.96$). Significantly differentially expressed genes (>twofold change and adjusted $P \leq 0.05$) were identified by comparing normalized gene expression levels in cells treated with PPD-coated beads (test treatment) versus cells treated with uncoated beads (PBS control treatment), taking into account the donor patient, to perform a paired analysis (Figure 4). A total of 1,206 genes were significantly differentially expressed in cells from healthy human control subjects, with 3,229 in the LTBI group. Strikingly, the molecular response to PPD-coated beads was attenuated in cells harvested from patients with sarcoidosis with only 352 differentially expressed genes.

Principal component analysis (PCA) using fold-change ratios in PBMCs (PPD versus PBS control treatment) revealed distinct patterns within the LTBI and sarcoidosis groups. In particular, PCA showed distinct clustering of four sarcoidosis samples from LTBI, whereas no distinct clustering was observed in normal, healthy control subjects (Figure 4A). Like PCA, Euclidean distance between samples was calculated to assess overall similarity between samples (Figure 4B). This analysis demonstrated a hierarchical clustering of four patients with sarcoidosis, whereas the

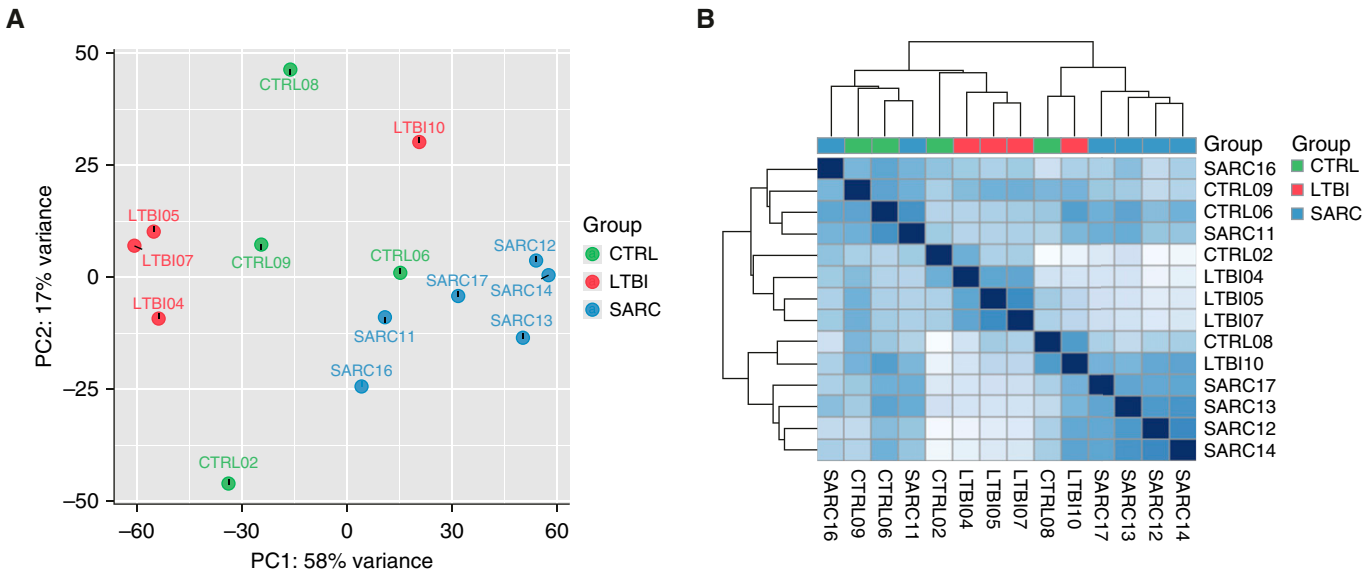


**Figure 4.** Clustering of global transcriptional responses of PBMCs after treatment with PPD-coated beads. (*A*) Principal component (PC) analysis of differential gene expression (AmpliSeq) performed on PBMCs derived from patients with SARC, LTBI, or normal healthy control subjects (CTRL) after incubation with PPD-coated beads for 7 days compared with paired treatment with uncoated (PBS-washed) beads. (*B*) Euclidean distance between samples was plotted to assess overall similarity between samples. This analysis revealed a hierarchical clustering of four subjects with SARC, whereas the remaining two SARC samples aligned more closely with CTRL (*see* text for further discussion).

remaining two sarcoidosis samples aligned more closely with controls. Of note, the two sarcoidosis samples that clustered with controls had lower cytokine production and developed less cell aggregation after PPD treatment compared with the other four subjects with sarcoidosis.

A more detailed comparison of gene expression patterns further differentiated sarcoidosis from LTBI. Table 3 provides a list of differentially expressed genes with the greatest fold change when comparing treatment with PPD-coated beads to correspondingly matched uncoated (PBS-washed) beads. The differentially expressed gene data used to generate the summary data in Table 3 are also represented graphically in the form of heat maps (Figure 5). This analysis indicated that PBMCs derived from the control and LTBI groups had a similar transcriptional response to PPD in some cases, whereas the sarcoidosis group had an attenuated response. For example, many transcripts exhibited similar patterns of expression in control subjects and those with LTBI (e.g., *GZMB*, *IFNG*, *SEPP1*, *CCL18*, *CD163*, *KIF2C*, *RASD1*, *TICRR*, *HIST1H2BB*, *RARRES1*, *STAB1*, *SEPP1*, and *ITGB5*). In contrast, none of these genes were significantly differentially expressed in the patients with sarcoidosis.

The relative change in gene expression, as reflected in Table 3, did not account for the absolute expression level of the transcripts or the statistical power of the observed changes in expression. These variables are accounted for in the "MvA" and "Volcano" plots when comparing treatment with PPD-coated beads to uncoated beads for the control, LTBI, and sarcoidosis groups (Figure 6).

## Discussion

The human *in vitro* granuloma model presented herein recapitulates several key features of tissue granulomas in sarcoidosis and LTBI, including three-dimensional cell aggregation, extracellular cytokine profiles, and induction of genes regulating molecular pathways characteristic of Th1 immune responses in the context of human granulomatous diseases. Moreover, and in contrast to models that had been previously developed and not widely adopted, the human *in vitro* model attributes are likely influenced by genetic variables that predispose to human granulomatous disease. The ability of the model to account for genetic variability is supported by the distinct molecular patterns that were promoted in human PBMCs in response to TB antigens in the sarcoidosis, LTBI, and normal, healthy control groups.

PBMC-based research is inherently convenient, but is also highly relevant for immunological research as it relates to granulomatous disorders. PBMCs constitute the reservoir from which most immune cells are recruited to the sites of new tissue granuloma formation. Furthermore, the maintenance of tissue granulomas is also dependent upon "new recruits" to maintain immune cell populations and to sustain coordinated interactions. Once recruited to the site of granuloma formation, the PBMCs become activated, as reflected by the production of various cytokines and chemokines, and in many cases, the cells further differentiate to play specific roles in the regulation of granulomatous inflammation (18–20). Investigations focused on *in vitro* immune responses to TB infection have yielded important discoveries relating to the pathogenesis of granulomatous diseases, including identification of *Mycobacterium tuberculosis* antigens essential for initial induction of granuloma formation (21), altered expression of host genes regulating type I IFNs, B and T cell functions in the context of active TB and LTBI (22), and the identification of microRNAs predicted to suppress WNT and transforming growth factor-β pathways in patients with sarcoidosis (23).

**Table 3.** The Most Significantly Differentially Expressed Genes Identified within the Granulomatous Structures in Each Donor Group 7 Days after Treatment, when Comparing Treatment with Purified Protein Derivative–Coated Beads to Correspondingly Matched Uncoated (PBS-Washed) Beads

| Gene | Accession No. | Fold Change | | |
|---|---|---|---|---|
| | | Control | LTBI | Sarcoid |
| Up-regulated genes | | | | |
| *IFNG* | NM_000619 | 156.8* | 239.7* | ns |
| *KIF2C* | NM_006845 | 50.5 | 189.3* | ns |
| *DMC1* | NM_007068 | 88.4* | 140* | 6.7 |
| *RASD1* | NM_016084 | 138* | 40.8 | ns |
| *TICRR* | NM_152259 | 25.4 | 131.2* | ns |
| *HIST1H2BB* | NM_021062 | 129* | 48.1 | ns |
| *ITGA2* | NM_002203 | 31.2 | 120.8* | ns |
| *DAPK2* | NM_014326 | 33.6 | 118.1* | ns |
| *ASPM* | NM_018136 | 38.6 | 108.8* | ns |
| *GZMB* | NM_004131 | 106.5* | 93.6* | 3.1 |
| *CDT1* | NM_030928 | 35.3 | 100.6* | ns |
| *DIAPH3* | NM_001042517 | 14.5 | 97.2* | ns |
| *CSF2* | NM_000758 | 83.1* | 35.7 | 12.8* |
| *CTLA4* | NM_005214 | 78.1* | 57.2 | 7.7 |
| *HIST1H3H* | NM_003536 | 74.2* | 65.7 | ns |
| *EGLN3* | NM_022073 | 74* | ns | ns |
| *INHBA* | NM_002192 | 69.9* | ns | ns |
| *CXCR6* | NM_006564 | 37.4 | 18.4 | 14.6* |
| *IL8* | NM_000584 | 7.4 | ns | 23.6* |
| *IL3RA* | NM_002183 | 22.7 | ns | 20.5* |
| *C21orf7* | NM_020152 | 5.4 | ns | 20.8* |
| *PTGES* | NM_004878 | ns | ns | 20.1* |
| *CRLF2* | NM_022148 | 6 | ns | 14.2* |
| *TNFAIP6* | NM_007115 | 5.3 | ns | 13.6* |
| *C1S* | NM_201442 | ns | ns | 13.1* |
| *CXCL5* | NM_002994 | ns | ns | 12* |
| Down-regulated genes | | | | |
| *RARRES1* | NM_206963 | −482.4* | −50.3 | ns |
| *STAB1* | NM_015136 | −333.2* | −174.9* | ns |
| *SEPP1* | NM_001085486 | −297.9* | −328.8* | ns |
| *LILRB5* | NM_001081442 | −66.2 | −275.1* | ns |
| *PMP22* | NM_153322 | −8.4 | −227.9* | ns |
| *ITGB5* | NM_002213 | −161.8* | −34.6 | ns |
| *CCL18* | NM_002988 | −159.2* | −99.5 | ns |
| *CD163* | NM_004244 | −93.7 | −158.3* | −3.6 |
| *FOLR2* | NM_001113536 | −137.1* | −105.8* | ns |
| *MMP12* | NM_002426 | −34.8 | −134* | ns |
| *HS3ST2* | NM_006043 | −111.4* | −124* | ns |
| *SPARC* | NM_003118 | −118.9* | −44 | ns |
| *MS4A6A* | NM_152851 | −60.1 | −117.4* | ns |
| *LPL* | NM_000237 | −108.6* | −38.4 | −7.7 |
| *MMP7* | NM_002423 | −38.1 | −108.3* | −3.1 |
| *MPEG1* | NM_001039396 | −106.3* | −51.5 | ns |
| *GAL* | NM_015973 | −50.5 | −30.2 | −11.6* |
| *TIMP3* | NM_000362 | −38.9 | −25.6 | −13.1* |
| *GALNT14* | NM_024572 | −37.5 | −30.3 | −11.8* |
| *CLMP* | NM_024769 | −13.4 | −29.9 | −18.3* |
| *FBLN5* | NM_006329 | −20.3 | −10 | −11.5* |
| *CACNA2D3* | NM_018398 | −19.9 | −16.8 | −14.5* |
| *S100A16* | NM_080388 | ns | ns | −18.8* |
| *GPER* | NM_001098201 | −16.7 | −10.3 | −14.9* |
| *HTR2B* | NM_000867 | ns | −9 | −12.9* |
| *GPD1* | NM_005276 | ns | ns | −10.5* |

*Definition of abbreviations*: LTBI, latent tuberculosis infection; ns, not significantly changed (i.e., $P > 0.05$).
Within each of the 3 treatment groups, the top 20 differentially expressed genes were identified (top 10 up- and 10 down-regulated); the resulting gene lists were merged.
*Differentially expressed genes falling within the top 10 of the given treatment group.

Despite similar granuloma-like appearance, the *in vitro* human granuloma model revealed significant distinctions in terms of the patterns of cytokine and gene expression in PBMCs from patients with sarcoidosis and LTBI, particularly in response to TB antigen stimulation. For instance, the release of IFN-γ was significantly higher after PPD treatment in LTBI, whereas relatively higher TNF-α expression was observed in sarcoidosis. In this regard, IFN-γ and TNF-α contribute independently to regulation of granulomatous immune responses. IFN-γ–mediated activation of signal transducer and activator of transcription (STAT) 1 transcription factor promotes immune responses that are critical for initial granuloma formation in response to infection (24, 25), and IFN-γ is essential to preventing dissemination of TB infection in mice (26), including prevention of reactivation of LTBI (27). In contrast, TNF-α is reportedly not essential for the initial granulomatous response to *M. tuberculosis* in mice, but is required for the maintenance of well formed granulomas and for eventual clearance of the pathogen (19).

It is interesting to consider the implications of higher production of TNF-α and the increased expression of other molecules engaged in antimicrobial functions (*IL8*, *CXCL1*, *CXCL3*, *CXCL5*, *CXCL16*, *CCL13*, *CCL18*, *MMP7*, *MMP12*, *MMP14*, *TLR2*, and *S100A8/S100A9*) in humans with sarcoidosis compared with patients with LTBI. For instance, significantly higher TNF-α production in patients with sarcoidosis is predicted to enhance bacterial and fungal pathogen clearance, which would reduce the risk of infections. On the other hand, excess TNF-α production in response to TB antigens may perpetuate granuloma formation in the absence of infection (by definition) in patients with sarcoidosis. In contrast to sarcoidosis, differential gene expression in LTBI included extremely high fold-change expressions of *IFNG* and *GZMB* (Table 3 and Figure 6), encoding molecules that are instrumental in the granulomatous immune response to TB in humans. This finding may reflect adaptation of the immune system to chronic low-grade TB infection, as previously reported (28, 29).

Gene expression analyses of the *in vitro* model may provide novel insights and new

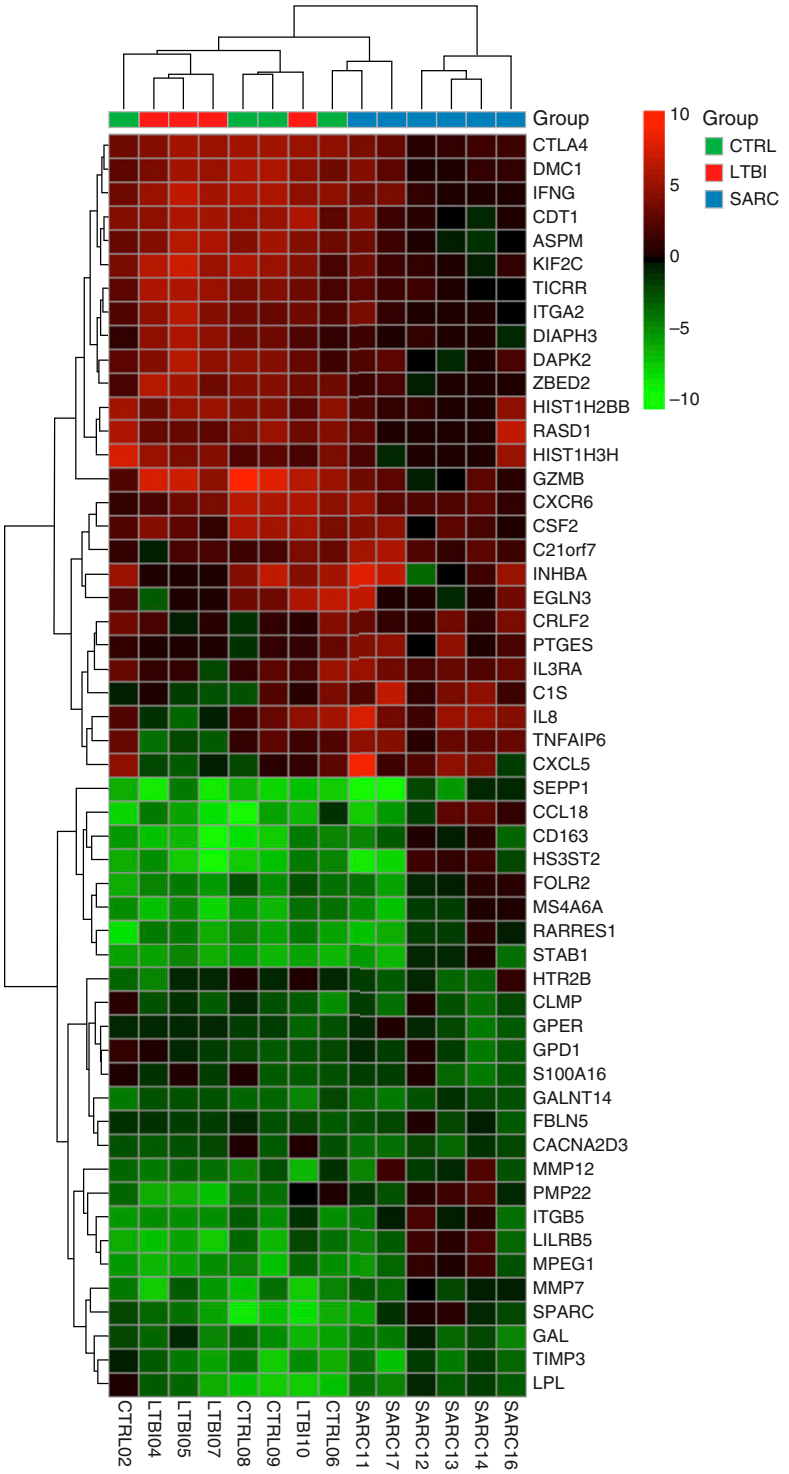


**Figure 5.** Heat map analysis of gene expression data from PPD-treated PBMCs. Differential gene expression was determined in PBMCs derived from patients with SARC, LTBI, or normal healthy control subjects (CTRL) after incubation with PPD-coated beads for 7 days compared with paired treatment with uncoated (PBS-washed) beads. The heat map was generated using the top 10 most up-regulated and top 10 most down-regulated genes within each treatment group. Genes with up-regulated expression are shaded *red*, whereas those with down-regulated expression are shaded *green*, based upon the magnitude of the change in expression. Hierarchical clustering demonstrated a grouping of four of six SARC samples, which were readily distinguished from three of four LTBI samples, based upon gene expression patterns (*see* text for further discussion).

hypotheses relating to disease mechanisms. Volcano plots of the transcriptional response to TB antigen in healthy control subjects (Figure 6B) and LTBI (Figure 6D) identified the genes with the highest statistical probability of differential expression, which included multiple genes coding for components of histone 1 (e.g., *HIST1H3H*, *HIST1H2BM*, *HIST1H2BB*, *HIST1H2BL*, *HIST3H2BB*, *HIST1H2AB*, *HIST1H3B*, and *HIST1H1A*), which were 40- to 140-fold up-regulated. In contrast, up-regulation of this group of genes was dramatically attenuated in sarcoidosis (two- to fivefold up-regulated). Lower expression (activity) of histone 1 has implications for the regulation of inflammatory and fibrotic responses (30, 31).

*S100A9* was observed to be significantly down-regulated at least 20-fold in both the control and LTBI groups, but expression remained unchanged in sarcoidosis. This increased relative expression of *S100A9* in the sarcoidosis group has been previously reported in sarcoidosis granulomas (32, 33), and is postulated to correspond with freshly recruited macrophages during the early phase of granuloma formation (34). Similarly, *CD163* expression was dramatically reduced (−58.8- and −52.5-fold in control subjects and LTBI, respectively), but was observed to be only moderately down-regulated in sarcoidosis (−5.8 fold), reflecting relative polarization to a M2 macrophage phenotype. M2 polarization has implications for promoting a fibrotic disease phenotype (i.e., poor prognosis) in patients with sarcoidosis (35).

Among the genes uniquely differentially expressed in LTBI in this model was *ABCA1* (−28.3-fold down-regulated), which is incriminated in the survival of macrophages and intracellular pathogens in the context of acute infection, presumably relating to the intracellular transport of cholesterol to maintain bacterial survival (36). The induction of *ABCA1* occurs within hours of infection in normal mice (36), whereas expression was greatly reduced by Day 7 in this model, suggesting that *ABCA1* expression was dynamically changing over time, or is perhaps fundamentally altered in patients with LTBI compared with those with active TB.

The nonspecific activation of sarcoidosis macrophages in response to

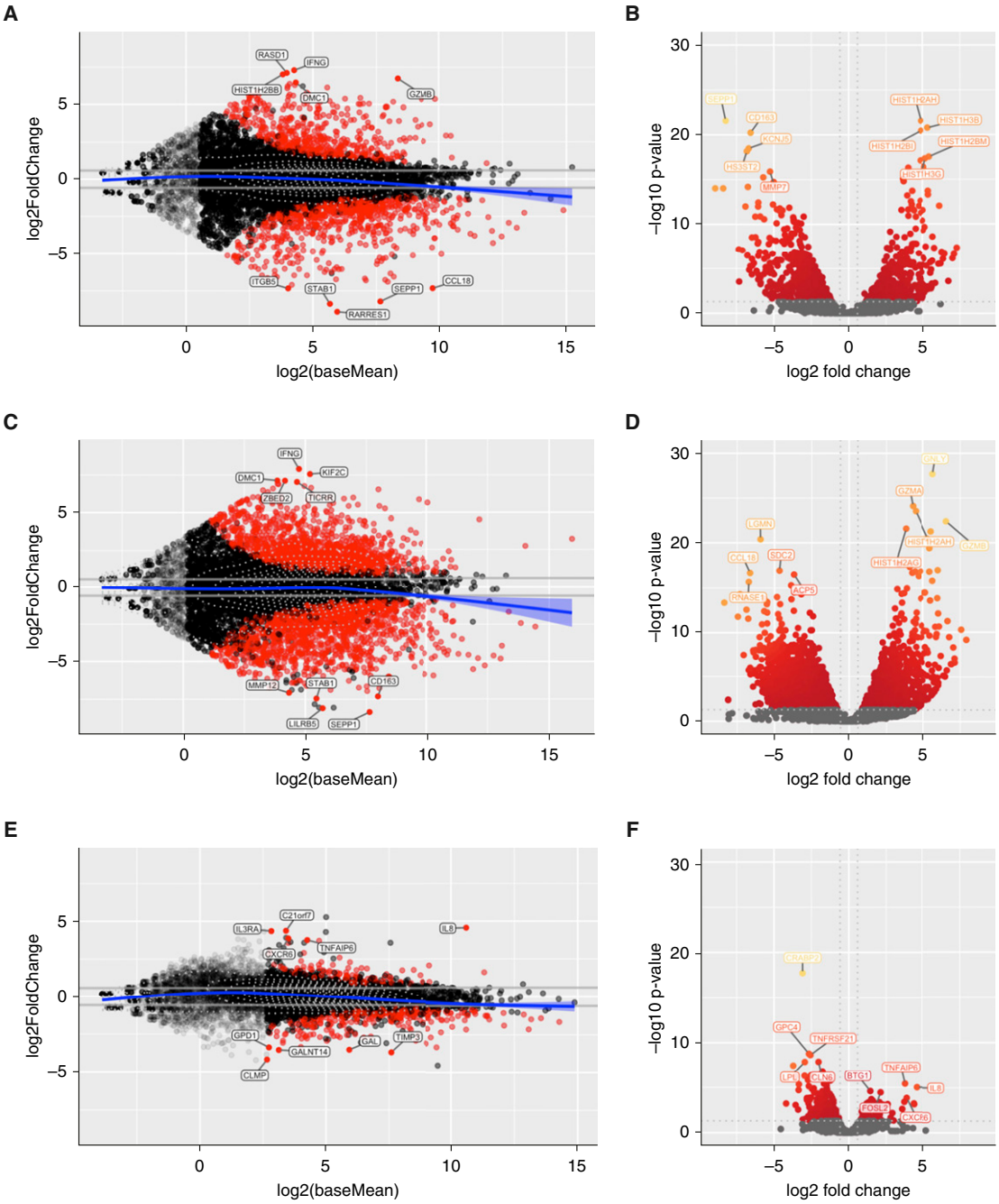


**Figure 6.** Gene expression comparison after PPD treatment of PBMCs derived from subjects with sarcoidosis, those with LTBI, and normal, healthy control subjects. The output type "MvA" plots are of normalized gene expression data wherein each point represents a gene, with the *y-axis* representing a log (base 2) fold change in expression after 7-day treatment with PPD-coated beads compared with uncoated beads for PBMCs derived from normal, healthy control subjects (*A*), subjects with LTBI (*C*), and subjects with sarcoidosis (*E*). The *x-axis* is the log average of the gene expression level. All genes with an adjusted *P* value of 0.05 (representing a 5% false discovery rate) and at least a twofold change (highlighted by the two *horizontal gray lines*) in the magnitude of gene expression between PPD and uncoated beads are shaded *red*. The *blue line* represents smoothed local mean expression (fitted using a generalized additive model), with the surrounding 95% confidence level interval shaded *light blue*. The *dotted gray contour lines* represent a two-dimensional density estimation. Genes most highly expressed in response to PPD-coated beads are highlighted in the *top* of the MvA plot, whereas those genes expressed at a lower level are at the *bottom* (the top five most differentially expressed genes in each case are labeled). Volcano plots of the same data wherein the *y-axis* corresponds with transcripts with high statistical significance (−log 10 of *P* value), and the *x-axis* corresponds with fold-change of gene expression (log base 2) were also generated for normal, healthy control subjects (*B*), subjects with LTBI (*D*), and those with sarcoidosis (*F*). Labeled transcripts on the *upper left side of the plot* have strong statistical significance with relatively low expression after treatment with PPD-coated versus uncoated beads. Transcripts on the *upper right* are more highly expressed with strong statistical significance after PPD treatment. The *dotted line* corresponds with a *P* value cutoff of 0.05, and genes failing to meet this cutoff are shaded *gray*.

HSA-coated beads observed herein is in keeping with previous reports of preactivated macrophages in patients with active pulmonary sarcoidosis (37, 38), including enhanced antigen-induced T cell activation (39). Moreover, prior studies have shown that blood macrophages derived from patients with sarcoidosis exhibit accelerated phagocytosis (40). The mechanisms by which HSA-coated beads promoted selective activation of the macrophages from patients with sarcoidosis are unclear.

We believe that the *in vitro* human granuloma model has the potential to rapidly advance discoveries in the fields of sarcoidosis, TB, and many other granulomatous diseases. One novel feature of the model is the opportunity to investigate disease mechanisms during the earliest phases of granuloma formation. For example, many genes regulated by IFN-γ/STAT1 signaling pathways were induced by PPD treatment in both sarcoidosis and LTBI PBMCs compared with controls. However, a subgroup of genes the expression of which remained unchanged in sarcoidosis in response to PPD antigens compared with significant down-regulation in LTBI (*CXCL16*, *MMP9*, *MMP12*) are specifically regulated by STAT1 through downstream transcription factors, interferon regulatory factor 8 (IRF8) (IRF8 expression was ∼ twofold higher in sarcoidosis compared with LTBI) and IRF1 (41, 42). Likewise, IFN-γ/STAT1 signaling and downstream nuclear transcription factors, Ikaros (expressed ∼ twofold higher in LTBI), cAMP response element-binding protein, and activator protein 1, regulate the transcription of *GZMB* (43), which was highly expressed in LTBI (but not in sarcoidosis) (Table 3). Thus, PPD activation led to distinct expression of IFN-regulated genes in human PBMCs derived from patients with sarcoidosis and LTBI. Future investigations using this model could consider genetic variables (e.g., *STAT1* [44] or *IRF8* [45] polymorphisms) or epigenetic factors (46) contributing to altered IFN-regulated responses in these patients.

As with any *in vitro* model, there are some limitations. It could be argued that PBMCs do not accurately represent the immune cell populations found in diseased tissues; however, most of the cells that ultimately contribute to tissue granuloma formation are derived from PBMCs (18–20, 47). This point was accentuated by the experimental data showing that chemokines made up the majority of the most highly expressed genes in PPD-induced granulomas in patients with sarcoidosis (Table 3). Another limitation is the lack of stromal cell support in the model. Stromal cells, particularly surrounding epithelial cells, contribute to macrophage recruitment to the granuloma in patients with TB (47), and increased stromal expression of a specific matrix metalloproteinase (a disintegrin and metalloproteinase domain-like protein decysin 1), a marker of monocyte differentiation (48), suggests a potential role in promoting pulmonary sarcoidosis granulomas (49). Nonetheless, as hypothesized, granuloma-like structures exhibiting molecular features previously reported in the context of diseased human tissues was demonstrated. Although the model does not account for all variables *in vivo*, it more closely approximates the complex interaction among immune cells during the early formation of granulomas in the context of sarcoidosis compared with existing laboratory models. In particular, this model is clearly more advanced in this regard compared with typical *in vitro* analyses involving a single cell line, which fails to account for dynamic immune cell interactions, which are the hallmark of granulomatous inflammation. This point is further emphasized by a preliminary analysis of gene expression data in the *in vitro* model compared with human tissue (Table E1) showing common differentially expressed gene expression characteristics. However, we are currently modifying the model to more closely replicate *in vivo* conditions by coculturing appropriate stromal cells during *in vitro* granuloma formation.

Another inherent limitation of sarcoidosis research is the lack of specific knowledge relating to disease-causing antigens. That said, previous studies show that approximately 60% of patients with sarcoidosis who are naive to TB infection respond abnormally to TB antigen challenge to promote an adaptive immune response (13), which is in keeping with the variable response to PPD-coated beads in this model (Figure 1). The study size was small, such that all sarcoidosis phenotypes were not likely to be represented. Nonetheless, two patterns emerged in the model that were in keeping with prior studies: four of six subjects with sarcoidosis studied herein were particularly high responders to PPD-coated beads in terms of *in vitro* granuloma formation and related Th1 molecular patterns (Figures 4 and 5). Furthermore, gene expression patterns of these four patients clustered together and were distinct from control subjects or subjects with LTBI after PPD-coated bead treatment. The remaining two patients with sarcoidosis clustered more closely with the control group (Figures 4 and 5). We had previously reported nonspecific accentuated Toll-like receptor (TLR) responses in patients with active sarcoidosis, including TLRs that are highly responsive to TB antigens (TLR2, TLR9) (50), leading us to conclude that patients with sarcoidosis would respond to other environmental challenges, such as propionibacterium (a TLR2 agonist) or DNA viruses (TLR9 agonists), as previously reported (51, 52). Furthermore, to more closely model the normal immune response to environmental antigens, which involves initial phagocytosis by antigen-presenting cells (dendritic cells, macrophages) and subsequent presentation of antigen to T cells, we used beads that are known to be processed by macrophages. Antigens loaded on beads are shown to be more efficient in forming productive immune synapses between macrophages and T cells and subsequent T cell activation and proliferation (53). Thus, we employed the antigen-coated beads (as opposed to soluble antigen) to more closely replicate the *in vivo* immune response wherein immunogenic antigens are often admixed with other environmental particles and to optimize antigen processing via phagocytosis and subsequent antigen presentation. Thus, the model will be useful for screening and validating environmental factors implicated in the pathogenesis of sarcoidosis (54).

The *in vitro* human granuloma model provides a novel research tool for exploring disease mechanisms and treatments in the context of sarcoidosis, TB, and, presumably, other human granulomatous disorders. The model incorporates key components of granuloma biology, including exposure to environmental antigens, highly variable host genetics, complex intracellular and intercellular signaling, and the variable of time, resulting in a model that, in several respects, replicates the human condition. As opposed to

research conducted on diseased human tissues, the model is highly versatile in that any number of variables can be manipulated, and it is relatively convenient and inexpensive compared with conventional studies based upon diseased tissues. Although not demonstrated here, the model is conducive to preclinical testing of existing or exploratory therapeutics designed to normalize the granulomatous response. ■

**Author disclosures** are available with the text of this article at www.atsjournals.org.

## References


1. Martin WJ II, Iannuzzi MC, Gail DB, Peavy HH. Future directions in sarcoidosis research: summary of an NHLBI working group. *Am J Respir Crit Care Med* 2004;170:567–571.
2. Nathan C, Barry CE III. TB drug development: immunology at the table. *Immunol Rev* 2015;264:308–318.
3. Myllymäki H, Niskanen M, Oksanen KE, Rämet M. Animal models in tuberculosis research—where is the beef? *Expert Opin Drug Discov* 2015;10:871–883.
4. Shultz LD, Ishikawa F, Greiner DL. Humanized mice in translational biomedical research. *Nat Rev Immunol* 2007;7:118–130.
5. Swaisgood CM, Oswald-Richter K, Moeller SD, Klemenc JM, Ruple LM, Farver CF, Drake JM, Culver DA, Drake WP. Development of a sarcoidosis murine lung granuloma model using *Mycobacterium* superoxide dismutase A peptide. *Am J Respir Cell Mol Biol* 2011;44:166–174.
6. Shi C, Shi J, Xu Z. A review of murine models of latent tuberculosis infection. *Scand J Infect Dis* 2011;43:848–856.
7. Newman KL, Newman LS. Occupational causes of sarcoidosis. *Curr Opin Allergy Clin Immunol* 2012;12:145–150.
8. Saunders BM, Britton WJ. Life and death in the granuloma: immunopathology of tuberculosis. *Immunol Cell Biol* 2007;85: 103–111.
9. Puissegur MP, Botanch C, Duteyrat JL, Delsol G, Caratero C, Altare F. An *in vitro* dual model of mycobacterial granulomas to investigate the molecular interactions between mycobacteria and human host cells. *Cell Microbiol* 2004;6:423–433.
10. Guirado E, Mbawuike U, Keiser TL, Arcos J, Azad AK, Wang SH, Schlesinger LS. Characterization of host and microbial determinants in individuals with latent tuberculosis infection using a human granuloma model. *MBio* 2015;6:e02537–14.
11. Co DO, Hogan LH, Il-Kim S, Sandor M. T cell contributions to the different phases of granuloma formation. *Immunol Lett* 2004;92: 135–142.
12. Girgis NM, Gundra UM, Ward LN, Cabrera M, Frevert U, Loke P. Ly6C(high) monocytes become alternatively activated macrophages in schistosome granulomas with help from $CD4^+$ cells. *PLoS Pathog* 2014;10:e1004080.
13. Song Z, Marzilli L, Greenlee BM, Chen ES, Silver RF, Askin FB, Teirstein AS, Zhang Y, Cotter RJ, Moller DR. Mycobacterial catalase-peroxidase is a tissue antigen and target of the adaptive immune response in systemic sarcoidosis. *J Exp Med* 2005;201:755–767.
14. Ellner JJ. Review: the immune response in human tuberculosis—implications for tuberculosis control. *J Infect Dis* 1997;176: 1351–1359.
15. Kapoor N, Pawar S, Sirakova TD, Deb C, Warren WL, Kolattukudy PE. Human granuloma *in vitro* model, for TB dormancy and resuscitation. *PLoS One* 2013;8:e53657.
16. Anders S, Huber W. Differential expression analysis for sequence count data. *Genome Biol* 2010;11:R106.
17. American Thoracic Society Joint Statement on Sarcoidosis. Statement on sarcoidosis: joint statement of the American Thoracic Society (ATS), the European Respiratory Society (ERS) and the World Association of Sarcoidosis and Other Granulomatous Disorders (WASOG) adopted by the ATS Board of Directors and by the ERS Executive Committee, February 1999. *Am J Respir Crit Care Med* 1999;160:736–755.
18. Khader SA, Rangel-Moreno J, Fountain JJ, Martino CA, Reiley WW, Pearl JE, Winslow GM, Woodland DL, Randall TD, Cooper AM. In a murine tuberculosis model, the absence of homeostatic chemokines delays granuloma formation and protective immunity. *J Immunol* 2009;183:8004–8014.
19. Roach DR, Bean AG, Demangel C, France MP, Briscoe H, Britton WJ. TNF regulates chemokine induction essential for cell recruitment, granuloma formation, and clearance of mycobacterial infection. *J Immunol* 2002;168:4620–4627.
20. Broos CE, van Nimwegen M, Hoogsteden HC, Hendriks RW, Kool M, van den Blink B. Granuloma formation in pulmonary sarcoidosis. *Front Immunol* 2013;4:437.
21. Parasa VR, Rahman MJ, Ngyuen Hoang AT, Svensson M, Brighenti S, Lerm M. Modeling *Mycobacterium tuberculosis* early granuloma formation in experimental human lung tissue. *Dis Model Mech* 2014;7:281–288.
22. Cliff JM, Kaufmann SH, McShane H, van Helden P, O'Garra A. The human immune response to tuberculosis and its treatment: a view from the blood. *Immunol Rev* 2015;264:88–102.
23. Crouser ED, Julian MW, Crawford M, Shao G, Yu L, Planck SR, Rosenbaum JT, Patrick Nana-Sinkam S. Differential expression of microRNA and predicted targets in pulmonary sarcoidosis. *Biochem Biophys Res Commun* 2012;417:886–891.
24. Bokhari SM, Kim KJ, Pinson DM, Slusser J, Yeh HW, Parmely MJ. NK cells and γ interferon coordinate the formation and function of hepatic granulomas in mice infected with the *Francisella tularensis* live vaccine strain. *Infect Immun* 2008;76:1379–1389.
25. Asano M, Nakane A, Minagawa T. Endogenous γ interferon is essential in granuloma formation induced by glycolipid-containing mycolic acid in mice. *Infect Immun* 1993;61:2872–2878.
26. MacMicking JD, Taylor GA, McKinney JD. Immune control of tuberculosis by IFN-γ–inducible LRG-47. *Science* 2003;302:654–659.
27. Scanga CA, Mohan VP, Joseph H, Yu K, Chan J, Flynn JL. Reactivation of latent tuberculosis: variations on the Cornell murine model. *Infect Immun* 1999;67:4531–4538.
28. Rozot V, Vigano S, Mazza-Stalder J, Idrizi E, Day CL, Perreau M, Lazor-Blanchet C, Petruccioli E, Hanekom W, Goletti D, *et al*. *Mycobacterium tuberculosis*-specific $CD8^+$ T cells are functionally and phenotypically different between latent infection and active disease. *Eur J Immunol* 2013;43:1568–1577.
29. Hassan SS, Akram M, King EC, Dockrell HM, Cliff JM. PD-1, PD-L1 and PD-L2 gene expression on T-cells and natural killer cells declines in conjunction with a reduction in PD-1 protein during the acute phase of tuberculosis treatment. *PLoS One* 2015;10:e0137646.
30. Li M, Liu X, Sun X, Wang Z, Guo W, Hu F, Yao H, Cao X, Jin J, Wang PG, *et al*. Therapeutic effects of NK-HDAC-1, a novel histone deacetylase inhibitor, on collagen-induced arthritis through the induction of apoptosis of fibroblast-like synoviocytes. *Inflammation* 2013;36:888–896.
31. Elsharkawy AM, Oakley F, Lin F, Packham G, Mann DA, Mann J. The NF-κB p50:p50:HDAC-1 repressor complex orchestrates transcriptional inhibition of multiple pro-inflammatory genes. *J Hepatol* 2010;53:519–527.
32. Delabie J, de Wolf-Peeters C, van den Oord JJ, Desmet VJ. Differential expression of the calcium-binding proteins MRP8 and MRP14 in granulomatous conditions: an immunohistochemical study. *Clin Exp Immunol* 1990;81:123–126.
33. Terasaki F, Fujita M, Shimomura H, Tsukada B, Otsuka K, Otsuka K, Katashima T, Ikemoto M, Kitaura Y. Enhanced expression of myeloid-related protein complex (MRP8/14) in macrophages and multinucleated giant cells in granulomas of patients with active cardiac sarcoidosis. *Circ J* 2007;71:1545–1550.
34. Kurata A, Terado Y, Schulz A, Fujioka Y, Franke FE. Inflammatory cells in the formation of tumor-related sarcoid reactions. *Hum Pathol* 2005;36:546–554.
35. Pechkovsky DV, Prasse A, Kollert F, Engel KM, Dentler J, Luttmann W, Friedrich K, Müller-Quernheim J, Zissel G. Alternatively activated alveolar macrophages in pulmonary fibrosis–mediator production and intracellular signal transduction. *Clin Immunol* 2010;137:89–101.

36. Stavrum R, Valvatne H, Stavrum AK, Riley LW, Ulvestad E, Jonassen I, Doherty TM, Grewal HM. *Mycobacterium tuberculosis* Mce1 protein complex initiates rapid induction of transcription of genes involved in substrate trafficking. *Genes Immun* 2012;13:496–502.
37. Strausz J, Männel DN, Pfeifer S, Borkowski A, Ferlinz R, Müller-Quernheim J. Spontaneous monokine release by alveolar macrophages in chronic sarcoidosis. *Int Arch Allergy Appl Immunol* 1991;96:68–75.
38. Fels AO, Nathan CF, Cohn ZA. Hydrogen peroxide release by alveolar macrophages from sarcoid patients and by alveolar macrophages from normals after exposure to recombinant interferons $\alpha$ A, $\beta$, and $\gamma$ and 1,25-dihydroxyvitamin D3. *J Clin Invest* 1987;80:381–386.
39. Venet A, Hance AJ, Saltini C, Robinson BW, Crystal RG. Enhanced alveolar macrophage–mediated antigen-induced T-lymphocyte proliferation in sarcoidosis. *J Clin Invest* 1985;75:293–301.
40. Dubaniewicz A, Typiak M, Wybieralska M, Szadurska M, Nowakowski S, Staniewicz-Panasik A, Rogoza K, Sternau A, Deeg P, Trzonkowski P. Changed phagocytic activity and pattern of Fc$\gamma$ and complement receptors on blood monocytes in sarcoidosis. *Hum Immunol* 2012; 73:788–794.
41. Dror N, Alter-Koltunoff M, Azriel A, Amariglio N, Jacob-Hirsch J, Zeligson S, Morgenstern A, Tamura T, Hauser H, Rechavi G, *et al*. Identification of IRF-8 and IRF-1 target genes in activated macrophages. *Mol Immunol* 2007;44:338–346.
42. Tamura T, Tailor P, Yamaoka K, Kong HJ, Tsujimura H, O'Shea JJ, Singh H, Ozato K. IFN regulatory factor-4 and -8 govern dendritic cell subset development and their functional diversity. *J Immunol* 2005; 174:2573–2581.
43. Wargnier A, Legros-Maida S, Bosselut R, Bourge JF, Lafaurie C, Ghysdael CJ, Sasportes M, Paul P. Identification of human granzyme B promoter regulatory elements interacting with activated T-cell–specific proteins: implication of Ikaros and CBF binding sites in promoter activation. *Proc Natl Acad Sci USA* 1995;92:6930–6934.
44. Tanaka G, Matsushita I, Ohashi J, Tsuchiya N, Ikushima S, Oritsu M, Hijikata M, Nagata T, Yamamoto K, Tokunaga K, *et al*. Evaluation of microsatellite markers in association studies: a search for an immune-related susceptibility gene in sarcoidosis. *Immunogenetics* 2005;56:861–870.
45. Salem S, Gros P. Genetic determinants of susceptibility to mycobacterial infections: IRF8, a new kid on the block. *Adv Exp Med Biol* 2013;783:45–80.
46. Coit P, Jeffries M, Altorok N, Dozmorov MG, Koelsch KA, Wren JD, Merrill JT, McCune WJ, Sawalha AH. Genome-wide DNA methylation study suggests epigenetic accessibility and transcriptional poising of interferon-regulated genes in naïve CD4$^+$ T cells from lupus patients. *J Autoimmun* 2013;43:78–84.
47. Ramakrishnan L. Revisiting the role of the granuloma in tuberculosis. *Nat Rev Immunol* 2012;12:352–366.
48. Fritsche J, Müller A, Hausmann M, Rogler G, Andreesen R, Kreutz M. Inverse regulation of the ADAM-family members, decysin and MADDAM/ADAM19 during monocyte differentiation. *Immunology* 2003;110:450–457.
49. Crouser ED, Culver DA, Knox KS, Julian MW, Shao G, Abraham S, Liyanarachchi S, Macre JE, Wewers MD, Gavrilin MA, *et al*. Gene expression profiling identifies MMP-12 and ADAMDEC1 as potential pathogenic mediators of pulmonary sarcoidosis. *Am J Respir Crit Care Med* 2009;179:929–938.
50. Julian MW, Shao G, Schlesinger LS, Huang Q, Cosmar DG, Bhatt NY, Culver DA, Baughman RP, Wood KL, Crouser ED. Nicotine treatment improves Toll-like receptor 2 and Toll-like receptor 9 responsiveness in active pulmonary sarcoidosis. *Chest* 2013;143: 461–470.
51. Dispenza MC, Wolpert EB, Gilliland KL, Dai JP, Cong Z, Nelson AM, Thiboutot DM. Systemic isotretinoin therapy normalizes exaggerated TLR-2–mediated innate immune responses in acne patients. *J Invest Dermatol* 2012;132:2198–2205.
52. Xu RH, Wong EB, Rubio D, Roscoe F, Ma X, Nair S, Remakus S, Schwendener R, John S, Shlomchik M, *et al*. Sequential activation of two pathogen-sensing pathways required for type I interferon expression and resistance to an acute DNA virus infection. *Immunity* 2015;43:1148–1159.
53. Olazabal IM, Martín-Cofreces NB, Mittelbrunn M, Martínez del Hoyo G, Alarcón B, Sánchez-Madrid F. Activation outcomes induced in naïve CD8 T-cells by macrophages primed via "phagocytic" and nonphagocytic pathways. *Mol Biol Cell* 2008;19: 701–710.
54. Liu H, Patel D, Welch AM, Wilson C, Mroz MM, Li L, Rose CS, Van Dyke M, Swigris JJ, Hamzeh N, *et al*. Association between occupational exposures and sarcoidosis: an analysis from death certificates in the United States, 1988–1999. *Chest* 2016;150: 289–298.